

# Zero-Compensation Method and Reduced Inductive Voltage Error for the AC Josephson Voltage Standard

Kunli Zhou, Jifeng Qu, and Samuel P. Benz, *Fellow, IEEE*

**Abstract**—In the pulse-driven ac Josephson voltage standard, the low frequency (LF) component of a drive signal increases the system complexity and induces unwanted voltages through on-chip inductances. A novel zero compensation (ZC) method for pulse-driven ac waveform synthesis is presented in this paper. A pulse train is obtained through a two-level  $\Delta$ - $\Sigma$  modulation and then reconstructed by replacing each pulse with three pulses of a negative–positive–negative pattern. The amplitudes of the reconstructed pulse train are carefully adjusted so that the positive pulses drive the Josephson junctions to the first quantum state, whereas the negative pulses keep the junctions on the zero quantum state and cancel the contribution of the positive pulses to the LF inductive voltage component. This new method eliminates the need for LF signal reinjection required by the conventional bias method and eliminates the need for a direct-current bias required by the recently proposed ZC method. An 8-kHz sinusoidal waveform with an amplitude of 1 mV rms is synthesized to demonstrate the feasibility of the approach. We also demonstrate that the inductive voltage error is significantly reduced for waveforms synthesized with the new method.

**Index Terms**—Digital–analog conversion, Josephson arrays, quantization, signal synthesis, standards, superconducting integrated circuits, voltage measurement.

## I. INTRODUCTION

THE ac Josephson voltage standard (ACJVS), or the Josephson arbitrary waveform synthesizer, has received increasing attention in metrology due to its high performance in synthesizing quantum-accurate voltages with a user-defined spectral distribution [1]–[5]. Conventionally, the ACJVS setup shown in Fig. 1(a) is used for waveform synthesis in which the pulse pattern is obtained using a three-level  $\Delta$ - $\Sigma$  modulation and then converted to high-speed pulses either by coupling a two-level code with a microwave signal [6] or by directly using a ternary pulse pattern generator (PPG) [7]. The generated positive and negative pulses drive the Josephson junctions (JJs) to the first positive and negative quantum states, respectively,

Manuscript received April 19, 2015; revised July 23, 2015; accepted August 9, 2015. Date of publication August 20, 2015; date of current version September 17, 2015. This work was supported by the National Natural Science Foundation of China under Grant 61372041 and Grant 61001034. This paper was recommended by Associate Editor O. Mukhanov.

K. Zhou is with the Department of Electrical Engineering, Tsinghua University, Beijing 100084, China, and also with the National Institute of Metrology, Beijing 100029, China.

J. Qu is with the National Institute of Metrology, Beijing 100029, China (e-mail: qujf@nim.ac.cn).

S. P. Benz is with the National Institute of Standards and Technology, Boulder, CO 80305 USA.

Color versions of one or more of the figures in this paper are available online at <http://ieeexplore.ieee.org>.

Digital Object Identifier 10.1109/TASC.2015.2470684

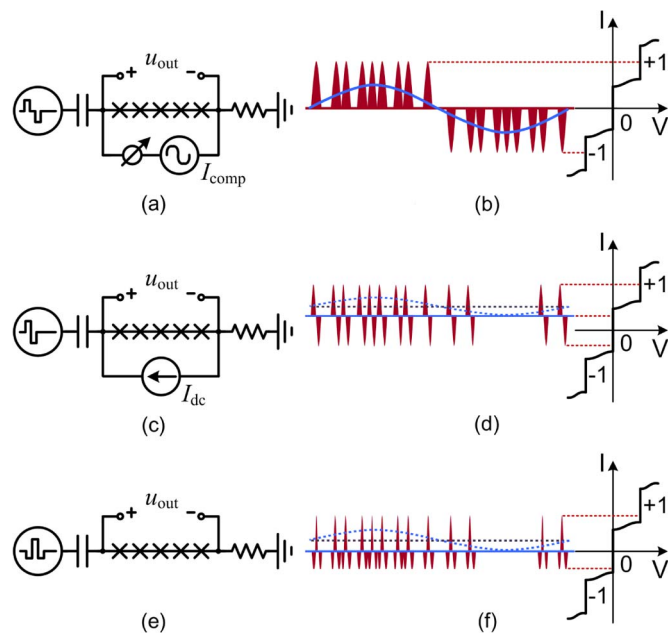


Fig. 1. (a)–(f) System setups and pulse-train biases for the three different pulse-bias methods. The HF bias is shown in red. The resulting LF and dc output voltages are shown as blue and black dashes, respectively. Note that the pulse widths in (b), (d), and (f) are the same for the three methods, which are determined by the output frequency of the ternary PPG. Here, they are differently plotted for schematic purposes. (a) Conventional. (b) Conventional. (c) ZC1. (d) ZC1. (e) ZC2. (f) ZC2.

as shown in Fig. 1(b). Note that the Shapiro steps of the current–voltage ( $I$ - $V$ ) curves in Fig. 1 are used to represent the first positive, zero, and first negative quantum states, which would be realized with a continuous stream of pulses with the corresponding polarity. A fast HF pulse train (colored in red) contains a LF component (colored in blue) that is dominated by the desired waveform [4].

To increase the output voltage, distributed arrays with multiple junctions connected in series are used for waveform synthesis [6]. On-chip microwave termination resistors are required for each JJ array to ensure that all the junctions have the same response. However, the LF component induces common-mode voltages on the termination resistors that are detrimental to the output waveform [6], [8]. Moreover, any common-mode signal on the terminations would hamper further attempts to increase the output voltage by connecting multiple arrays in series. To address these problems, filtering out the LF component in a pulse-bias signal is typically accomplished with a series of dc blocks and attenuators inserted in the pulse transmission path. Nevertheless, the removed LF component determines the shape

of the pulse train; thus, the train without the LF component cannot produce operating margins, except for the smallest synthesized voltages ( $\sim 5\%$ – $10\%$  of the  $n = 1$  quantum state) [8]. Usually, an arbitrary waveform generator (AWG) that is synchronized to the PPG pattern reinjects the LF component as a *compensation* bias current to each Josephson array to recover the LF component and to achieve operating margins [4]–[6], [8].

The LF component affects the system performance in two aspects. First, the reinjection of the LF component increases the experimental complexity. During system operation, one AWG is required to bias each Josephson array, and the AWG LF bias amplitude and relative phase (with respect to the PPG bias) are parameters that must be adjusted to optimize the operating margin of each array for each synthesized waveform [4]–[6], [8]. These two parameters increase the system complexity, particularly for two or more arrays connected in series, due to the increased number of bias parameters that need to be adjusted. An autoadjustment method was proposed by Brom and Houtzager [4] to search the optimal operating parameters with higher efficiency. Second, the LF component flows across any on-chip inductances, such as the transmission line and Josephson inductances, and it induces unwanted voltages. This frequency-dependent component adds to the synthesized quantum voltage in quadrature and must be accounted for to determine the accuracy of the output voltage, particularly for high frequencies [4], [9].

Recently, Benz *et al.* have proposed a zero compensation (ZC) method to eliminate the reinjection of the LF component [10]–[12]. This method successfully eliminated the ac compensation bias signal required to achieve operating margins, but it still required a dc-bias current [10] to produce the desired quantum voltages. In this paper, we propose a novel ZC approach that further simplifies the system configuration by eliminating the need for both the dc and LF compensation biases. The method will find an application in which higher accuracy or simpler system configurations are required, e.g., the measurement of the Boltzmann constant with Johnson noise thermometry [13], [14]. We synthesized a sinusoidal waveform of 1 mV rms by driving a JJ array containing 6400 junctions at a 4.99968-GHz clock frequency to demonstrate the feasibility of the proposed ZC approach. Moreover, the inductive voltage error in the synthesized waveform is measured and compared with that obtained from the conventional method. The results indicate that the inductive voltage errors are significantly reduced for waveforms synthesized with the ZC methods.

## II. ZC METHODS

With the ZC method proposed by Benz and Waltman in [10], which is named ZC1, the pulse pattern is obtained through a two-level  $\Delta$ – $\Sigma$  modulation, and then, the bit sequence is reconstructed by transforming each of the two levels of a single bit into a pair of bits, i.e., either 01 or 10. When combined with a dc-offset current and a microwave signal of appropriate phase and frequency that is half of the nonreturn-to-zero clock frequency, one of these bit pairs effectively produces no pulses. In this paper, a ternary PPG (BPG12G-TER from Symplis)

delivering return to zero (RZ) pulses is used for waveform synthesis.<sup>1</sup> One advantage of a ternary PPG is that no phase adjustment is required with a continuous-wave bias signal.

In Fig. 1(c) and (d), we show a bias scheme and a pulse schematic that closely resembles the ZC1 method in [10] but is realizable with our ternary PPG. After the two-level  $\Delta$ – $\Sigma$  modulation, unipolar pulses are transformed by replacing each positive pulse with a positive–negative pulse pair. In this bias scheme, an additional dc bias is necessary, as described in [10], to ensure that the junctions only produce positive pulses. Thus, the positive pulses of the resulting three-level (positive, zero, and negative) pulse-bias sequence represent the expected voltage waveform produced by the junctions. The LF component in the positive-pulse train is expected to be completely canceled by the opposite polarity pulses, provided that the areas of both polarities of the pulses are identical. The result is that each JJ toggles between the zero and first quantum states. This dc-bias current source still increases the system complexity that limits its application, e.g., in the quantum-voltage-calibrated Johnson noise thermometry [13], [14].

Another advantage of the ternary PPG is that the amplitudes of the positive and negative pulses can be adjusted independently. This enables us to propose the new ZC method shown in Fig. 1(e) and (f), i.e., ZC2, which eliminates the dc-bias current and further simplifies the ACJVS setup. After the expected waveform is digitized by the two-level  $\Delta$ – $\Sigma$  modulation, we perform a one-to-three-bit transformation, as opposed to the one-to-two-bit transformation for the ZC1 method in [10] and in Fig. 1(c) and (d). In this new bias scheme, the second digital signal of opposite polarity is used to produce a pair of negative pulses so that each positive pulse in the code pattern is replaced by a negative–positive–negative pulse sequence. When the amplitudes of the two negative pulses are precisely half those of the positive pulse, the LF component of this ternary-level bitstream with three-bit encoding is significantly reduced.

To drive the JJ array, both the positive pulses and the half-amplitude double-negative pulses are adjusted to optimize operating margins and to minimize the LF component of the bitstream. Because the half-amplitude of the negative pulses is insufficient to cause the JJs to pulse negatively, each three-bit sequence (negative–positive–negative pulses) has the same effect, as in [10], such that each JJ only produces one positive pulse without a dc-bias current.

These two ZC methods share two disadvantages. First, the maximum output voltage is reduced. The JJs primarily operate in the zero and positive first quantum states to produce the desired voltages; this unipolar output of both methods reduces the maximum output voltage by a factor of two compared with that for the conventional method, in which both negative and positive first quantum states are used. In addition, the one-to-two or one-to-three pulse transformation reduces the effective sampling frequency by twofold or threefold. Since the maximum output voltage is also proportional to the sampling

<sup>1</sup>Commercial instruments are identified in this paper in order to adequately specify the experimental procedure. Such identification does not imply recommendation or endorsement by NIST, nor does it imply that the equipment identified is necessarily the best available for the purpose.

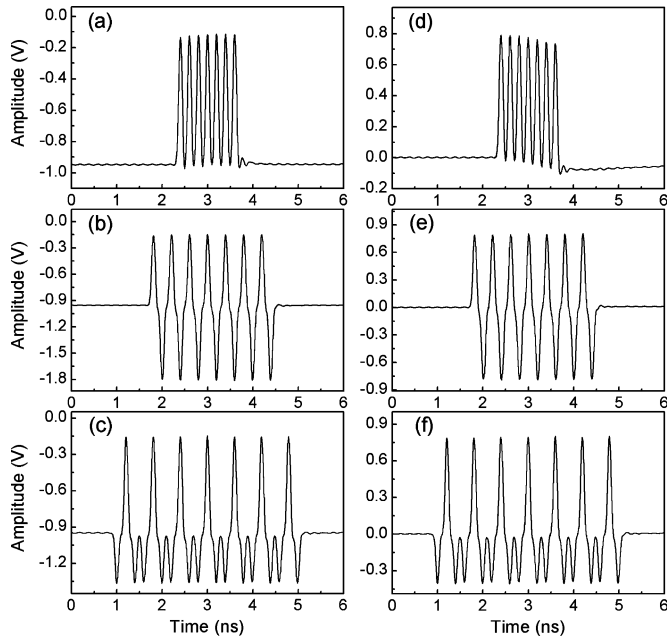


Fig. 2. Pulse trains generated by the ternary PPG (a)–(c) before and (d)–(f) after high-pass filtering by a 0.25–18-GHz dc block for the three different methods. (a) Conventional. (b) ZC1. (c) ZC2. (d) Conventional. (e) ZC1. (f) ZC2.

frequency, in comparison with the conventional method, there is an overall reduction in the maximum output voltage by a factor of 4 and 6 for the ZC1 and ZC2 methods, respectively. Recently, Benz *et al.* at the National Institute of Standards and Technology (NIST) [11], [12] and Kieler *et al.* at the Physikalisch-Technische Bundesanstalt (PTB) [15] have both demonstrated a rms output voltage of 1 V using the conventional method with the reinjection of the LF component. Four arrays with 12 800 junctions in each array at NIST [12] are required. To achieve a rms output voltage of 1 V with the ZC methods, 16 and 24 arrays will be necessary for the ZC1 and ZC2 methods, respectively.

The other disadvantage of the ZC methods is that the synthesized waveform contains a dc voltage, as shown in Fig. 1(d) and (f). Fortunately, this component can be canceled out by driving another array in series to synthesize a waveform with opposite polarity of the dc component [10], [12]. This was experimentally demonstrated in [12], where a sinusoidal waveform of 128 mV rms with no dc offset was synthesized by connecting two arrays in series using the ZC1 method.

To demonstrate the feasibility of the proposed method and the reduction of the LF component, the three methods shown in Fig. 1 were compared in both the time and frequency domains. Fig. 2 shows the measured pulse-bias signals generated by the PPG before [see Fig. 2(a)–(c)] and after [see Fig. 2(d)–(f)] high-pass filtering by a 0.25–18-GHz inner dc block. Note that the waveform in Fig. 2(a) contains LF components. After filtering by the dc block, the amplitudes of the pulses are reduced, as shown in Fig. 2(d). However, for the two ZC waveforms shown in Fig. 2(b) and (c), the LF components are very small that the dc block has negligible impact on the pulse amplitudes [see Fig. 2(e) and (f)].

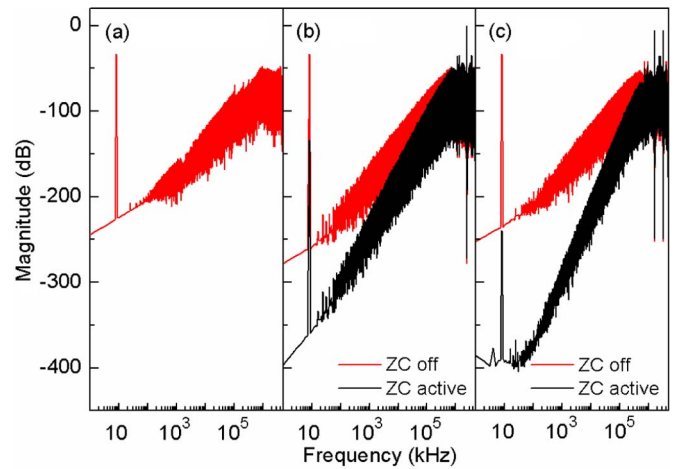


Fig. 3. (a)–(c) FFT spectra of the digital codes for the three different methods. The black and red lines in (b) and (c) correspond to the codes with the ZC active and off, respectively. (a) Conventional. (b) ZC1. (c) ZC2.

The sinusoidal waveforms with the same amplitude of 1 mV rms at a frequency of 8 kHz were synthesized by driving an array of 6400 JJs with the three different methods. For the conventional method, the sinusoidal waveform of eight periods is sampled at a rate  $f_s = 4.99968$  GHz that is close to the maximum output frequency of the BPG12G-TER, which results in  $N_s = 4\,999\,680$  samples. A three-level second-order  $\Delta$ – $\Sigma$  modulation is then performed to get the digital code corresponding to the pulse train that is used to drive the JJs. The corresponding pulse density in the  $\Delta$ – $\Sigma$  modulation code is about 2%. For the two ZC methods, the sampling rates used to digitize the waveform are respectively reduced to  $f_s/2$  and  $f_s/3$ , and the bit lengths are reduced to  $N_s/2$  and  $N_s/3$ , respectively. Their pulse densities are about 9% and 13%, respectively. The resulting codes produced by the two-level second-order  $\Delta$ – $\Sigma$  modulation are then encoded by replacing a “1” pulse with either a “1/–1” pair of pulses or a “–1/1/–1” triplet of pulses for the two ZC methods. The resulting transformed and encoded pulse outputs for the three respective bias schemes all have the same output pulse rate  $f_s$  and pulse length  $N_s$  that are used to drive the JJs.

Fig. 3 compares the spectra of the fast Fourier transform (FFT) of each of the digital codes for the three methods. Fig. 3(a) is the spectrum of the three-level code for the conventional method. In Fig. 3(b) and (c), the red lines correspond to the FFTs of only the positive pulses (replacing each “–1” by “0”) of the codes for the ZC1 and ZC2 methods, respectively. One can see that the expected 8-kHz tones have the same amplitude in all of the three red spectra. Note that the quantization noise floor at a fundamental frequency of 8 kHz in the red spectra for the ZC1 and ZC2 methods is slightly lower than that for the conventional method. This can be attributed to the different code levels and to the different sampling frequencies used in the  $\Delta$ – $\Sigma$  modulation. Note also that the dc offsets for the ZC1 and ZC2 methods are about 16.5 and 11.0 mV, respectively, which are not shown in Fig. 3(b) and (c). The black spectrum in Fig. 3(b) is calculated from the digital code for the ZC1 method. The spectrum for the ZC2 method

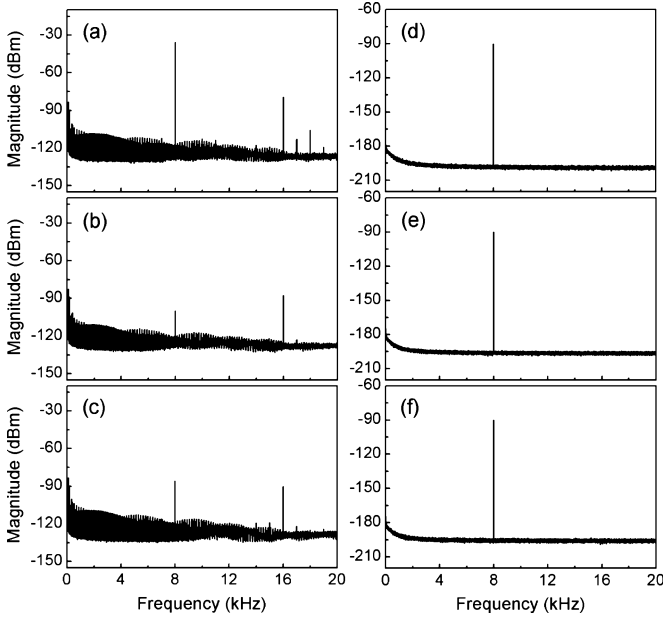


Fig. 4. (a)–(c) Measured spectra of the pulse-bias signals before filtering by the dc blocks for the three different methods. (d)–(f) Corresponding quantized 8-kHz synthesized sinusoidal waveforms with an amplitude of 1 mV rms. The input range of the digitizer NI PXI 5922 is 2 V, and the input impedances are 50  $\Omega$  for the bias signal measurements in (a)–(c) and 1 M $\Omega$  for the quantum voltage measurements in (d)–(f). (a) Conventional. (b) ZC1. (c) ZC2. (d) Conventional. (e) ZC1. (f) ZC2.

[the black line in Fig. 3(c)] is found by calculating the FFT of the digital code, with each “–1” replaced with a “–0.5” since the negative pulses should be half the amplitude of the positive pulses. Note that the amplitudes of the 8-kHz harmonic signals are significantly reduced for both ZC methods [the black FFTs in Fig. 3(b) and (c)], but they are not completely eliminated due to the conversion error inherent in the  $\Delta$ – $\Sigma$  modulator.

Fig. 4 shows the measured spectra of the pulse trains before they become filtered by the dc blocks and the corresponding synthesized quantum waveforms acquired by a high-performance spectrum analyzer (NI PXI 5922). In Fig. 4(a)–(c), one can see that, compared with the conventional method [see Fig. 4(a)], the LF component at a fundamental frequency of 8 kHz in the pulse train is significantly reduced by about 64.4 and 50.3 dB for the ZC1 and ZC2 methods, respectively. However, all three methods produce quantized sine waves of identical amplitude at 8 kHz and extremely low-harmonic distortions, as shown in Fig. 4(d)–(f). Note that the encoded waveforms of each bias method produce different quantum states. For example, for the conventional method, the JJs produce waveforms with bipolar pulses (+1/0/–1), whereas waveforms with unipolar pulses (+1/0) are produced by the junctions for both of the ZC methods.

There are two aspects worthy of further discussion for the aforementioned experiments. First, in Fig. 3, the reduction of the LF component for the ZC2 method is more significant than that for the ZC1 method. However, the situation is reversed in Fig. 4. This difference is attributed to the nonlinearities of the ternary PPG. Second, the operating margins are slightly different, i.e., about 0.44, 0.58, and 0.69 mA for the conventional, ZC1, and ZC2 methods, respectively. Note that the reinjection

of the LF component is not applied here for the conventional method. The effect shown in Fig. 2(d) is the main reason that the operating margin for the conventional method is smaller than those for the two ZC methods. With the reinjection of the LF component, the margin would be larger. Furthermore, the characteristic frequency of the JJs is about 15 GHz. Since the maximum output frequency of the BPG12G-TER is limited to around 5 GHz, the operating margins reported here are smaller than the margins demonstrated in [10] because we drove the junctions at 1/3 of the junction characteristic frequency. We expect that larger operating margins could be demonstrated using this array if we use a bit sequence that was RZ clocked at 15 GHz. In addition, for the ZC methods, the operating margins could be further increased by the use of a first-order  $\Delta$ – $\Sigma$  modulation [10], but these synthesized waveforms would have slightly higher quantization noise.

### III. REDUCED INDUCTIVE VOLTAGE ERROR

When synthesizing waveforms with the ACJVS, the accuracy of the output voltage will be decreased by the inductive voltage introduced by the LF component flowing across the combined inductance of the Josephson array circuit, which includes the inductance of the transmission line and the junctions. The inductive voltage is a dominant error for frequencies above 20 kHz and affects the total output voltage in the form of a voltage component orthogonal in phase to the quantum-accurate voltage signal produced by the JJs [9]. Estimating or measuring its contribution to the total output voltage is necessary, particularly for high frequencies. However, because it shares the same frequency with the fundamental synthesized signal, a direct measurement is difficult.

A two-step process is used to quantify the inductive voltage error, which was previously discussed in [16]. First, we reduced the amplitudes of the bias parameters to ensure that the JJs are biased at zero voltage, i.e., in the zero quantum state, in which case the JJs do not generate quantized pulses. The voltage measured at the JJ array output is exactly inductive voltage  $V_{\text{induc}0}$  for the reduced-amplitude bias current. To get a measurable signal, the patterns calculated from the conventional method are used for the  $V_{\text{induc}0}$  measurement. Second, we tuned the bias parameters to the values that allow the normal operation of the JJs. Thus, the inductive voltage  $V_{\text{induc}1}$  in the second step could be inferred from the scaling of the bias parameters as follows:

$$V_{\text{induc}1} = \frac{I_1}{I_0} V_{\text{induc}0} \quad (1)$$

where  $I_0$  and  $I_1$  are the LF bias currents when the JJs are biased on the zero and first quantum states, respectively.

The contribution of  $V_{\text{induc}1}$  can be expressed as the square of the voltage ratio  $R$  relative to the desired quantum voltage  $V_1$  as follows:

$$R = \left( \frac{V_{\text{induc}1}}{V_1} \right)^2. \quad (2)$$

The waveform patterns corresponding to voltages of different amplitudes ranging from 0.5 to 3.5 mV with a step of 0.5 mV and different frequencies ranging from 400 kHz to 1.8 MHz with a step of 200 kHz are used to produce the corresponding

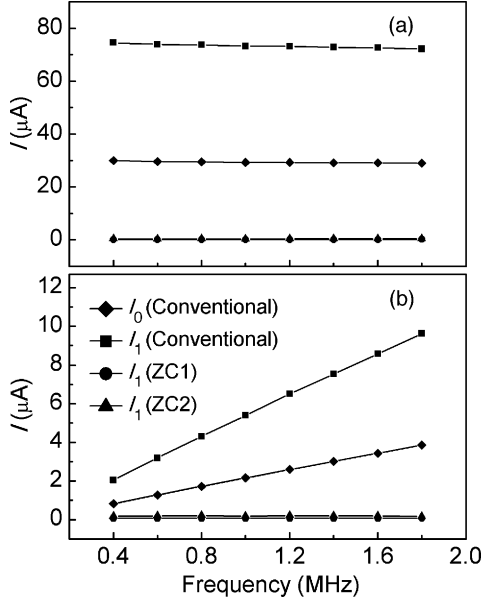


Fig. 5. Measured bias current (a) before and (b) after filtering by the dc blocks when the JJs are driven to the zero and first quantum states for waveforms of 1 mV rms amplitude and different frequencies. The input range and input impedance of the digitizer NI PXI 5922 are 2 V and 50  $\Omega$ , respectively.

different bias currents. The patterns are loaded into the PPG memory, and its output is connected to the digitizer NI PXI 5922 with an input impedance of 50  $\Omega$  to measure the bias currents. Fig. 5 shows the measured bias currents for waveform patterns of 1 mV rms amplitude and different frequencies before and after filtering by one 0.25–18-GHz inner dc block and one 0.01–18-GHz inner and outer dc block when the JJs operate in the zero or the first quantum state. The bias currents are approximately independent of the frequency before filtering by the dc blocks. However, due to the nonflat stopband frequency response of the dc blocks, bias currents  $I_0$  and  $I_1$  linearly increase with the frequency for the conventional method [the diamonds and squares in Fig. 5(b)]. For the two ZC methods, because bias currents  $I_1$  have been already reduced to rather small values in the original signals [the circles and triangles in Fig. 5(a)], they seem independent of the frequency after filtering by the dc blocks [the circles and triangles in Fig. 5(b)].

Fig. 6(a) shows the frequency dependence of the measured inductive voltage contribution  $V_{\text{induc}0}$  and the calculated inductive voltage contribution  $V_{\text{induc}1}$  for the three methods. Since the inductive impedance is a first-order function of the frequency, as a result, inductive voltages  $V_{\text{induc}0}$  and  $V_{\text{induc}1}$  for the conventional method increase as the frequency squared. For the two ZC methods,  $V_{\text{induc}1}$  is very small and practically independent of the frequency [the circles and triangles in Fig. 6(a)].

The averaged result for waveforms with different voltages was used to calculate power ratio  $R$ , as shown in Fig. 6(b). Fractional power  $R$  for the two ZC methods is significantly smaller than that for the conventional method, demonstrating again that the inductive voltage errors are greatly reduced for the two ZC methods due to the smaller LF bias current. For the conventional method [the squares in Fig. 6(b)], the contribution of the inductive voltage in power is about  $1 \times 10^{-6}$

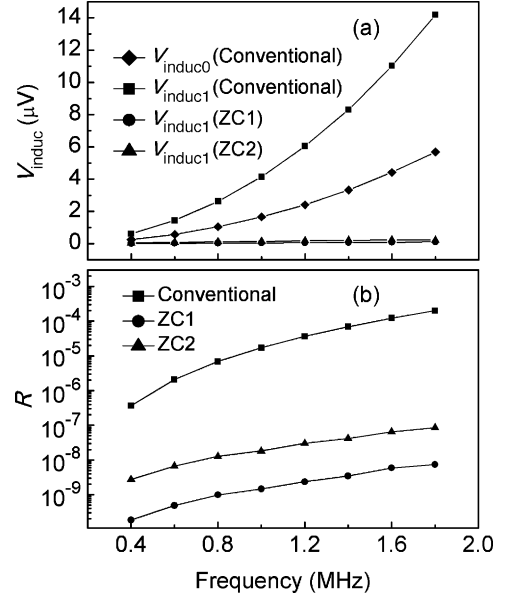


Fig. 6. (a) Measured inductive voltage  $V_{\text{induc}0}$  and calculated inductive voltage  $V_{\text{induc}1}$  for waveforms of different frequencies when the JJs are driven to the zero and first quantum states, respectively. (b) Calculated power ratio for the three different methods.

at 500 kHz that corresponds to a relative voltage error of about 0.5  $\mu\text{V}/\text{V}$ , provided that the inductive voltage is added to the synthesized waveform orthogonally. It becomes even larger at higher frequencies (about 100  $\mu\text{V}/\text{V}$  at 1.8 MHz). For both the ZC methods, the inductive voltage signals are reduced by more than 30 dB as compared with that produced by the conventional method. Fractional power  $R$  is less than  $9 \times 10^{-8}$ , even at 1.8 MHz, which corresponds to a voltage error less than 0.045  $\mu\text{V}/\text{V}$ . Again, for the conventional method, no LF reinjection was applied in the measurements. With the reinjection of the LF component, the inductive error would be significantly larger.

#### IV. CONCLUSION AND DISCUSSIONS

Sinusoidal waveforms of 8-kHz frequency and 1 mV rms amplitude with practical operating margins were successfully synthesized using three different bias methods, i.e., the conventional method, the binary-transformed ZC method with a dc-bias current [10], and a novel ternary-transformed ZC method that eliminates the need for both the LF compensation and dc-bias currents. The measurements of the synthesized signal generated with both the ZC methods show that the LF components are almost negligible in the pulse train that drives the JJ array and that the resulting inductive voltage errors are significantly reduced in the synthesized quantum voltage waveform.

For metrological applications, it is important to perform verification measurements with, for example, a thermal transfer standard at different frequencies, particularly at high frequencies, to verify the accuracy of the synthesized waveforms with the ZC methods. Moreover, besides the inductive voltage error, the accuracy of the synthesized waveforms is also influenced by other error sources, including input/output coupling, the effects of the transmission lines, and other systematic error sources. We

will perform such measurements and provide the corresponding analyses in a future paper.

#### ACKNOWLEDGMENT

The authors would like to thank P. D. Dresselhaus and C. J. Burroughs for the chip fabrication and packaging.

#### REFERENCES

- [1] S. P. Benz and C. A. Hamilton, "A pulse-driven programmable Josephson voltage standard," *Appl. Phys. Lett.*, vol. 68, no. 22, pp. 3171–3173, May 1996.
- [2] P. S. Filipinski, M. Boecker, S. P. Benz, and C. J. Burroughs, "Experimental determination of the voltage lead error in an ac Josephson voltage standard," *IEEE Trans. Instrum. Meas.*, vol. 60, no. 7, pp. 2387–2392, Jul. 2011.
- [3] N. Kaneko, M. Maruyama, and C. Urano, "Current status of Josephson arbitrary waveform synthesis at NMIJ/AIST," *IEICE Trans. Electron.*, vol. E94-C, no. 3, pp. 273–279, Mar. 2011.
- [4] H. E. van den Brom and E. Houtzager, "Voltage lead corrections for a pulse-driven ac Josephson voltage standard," *Meas. Sci. Technol.*, vol. 23, no. 12, Dec. 2012, Art. ID. 124007.
- [5] O. F. O. Kieler, R. P. Landim, S. P. Benz, P. D. Dresselhaus, and C. J. Burroughs, "AC-DC transfer standard measurements and generalized compensation with the ac Josephson voltage standard," *IEEE Trans. Instrum. Meas.*, vol. 57, no. 4, pp. 791–796, Apr. 2008.
- [6] S. P. Benz, C. J. Burroughs, and P. D. Dresselhaus, "AC coupling technique for Josephson waveform synthesis," *IEEE Trans. Appl. Supercond.*, vol. 11, no. 1, pp. 612–616, Mar. 2001.
- [7] H. E. van den Brom, E. Houtzager, B. E. R. Brinkmeier, and O. A. Chevtchenko, "Bipolar pulse-drive electronics for a Josephson arbitrary waveform synthesizer," *IEEE Trans. Instrum. Meas.*, vol. 57, no. 2, pp. 428–431, Feb. 2008.
- [8] S. P. Benz, P. D. Dresselhaus, C. J. Burroughs, and N. F. Bergren, "Precision measurements using a 300 mV Josephson arbitrary waveform synthesizer," *IEEE Trans. Appl. Supercond.*, vol. 17, no. 2, pp. 864–869, Jun. 2007.
- [9] C. J. Burroughs, S. P. Benz, and P. D. Dresselhaus, "AC Josephson voltage standard error measurements and analysis," *IEEE Trans. Instrum. Meas.*, vol. 52, no. 2, pp. 542–544, Apr. 2003.
- [10] S. P. Benz and S. B. Waltman, "Pulse-bias electronics and techniques for a Josephson arbitrary waveform synthesizer," *IEEE Trans. Appl. Supercond.*, vol. 24, no. 6, Dec. 2014, Art. ID. 1400107.
- [11] S. P. Benz, *et al.*, "One-volt Josephson arbitrary waveform synthesizer," *IEEE Trans. Appl. Supercond.*, vol. 25, no. 1, Feb. 2015, Art. ID. 1300108.
- [12] S. P. Benz, *et al.*, "Performance improvements for the NIST 1 V Josephson arbitrary waveform synthesizer," *IEEE Trans. Appl. Supercond.*, vol. 25, no. 3, Jun. 2015, Art. ID. 1400105.
- [13] J. Qu, *et al.*, "Flat frequency response in the electronic measurement of Boltzmann's constant," *IEEE Trans. Instrum. Meas.*, vol. 62, no. 6, pp. 1518–1523, Jun. 2013.
- [14] D. R. White, "Non-linearity in Johnson noise thermometry," *Metrologia*, vol. 49, no. 6, pp. 651–665, Dec. 2012.
- [15] O. F. Kieler, *et al.*, "Towards a 1 V Josephson arbitrary waveform synthesizer," *IEEE Trans. Appl. Supercond.*, vol. 25, no. 3, Jun. 2015, Art. ID. 1400305.
- [16] R. P. Landim, S. P. Benz, P. D. Dresselhaus, and C. J. Burroughs, "Systematic-error signals in the ac Josephson voltage standard: Measurement and reduction," *IEEE Trans. Instrum. Meas.*, vol. 57, no. 6, pp. 1215–1220, Jun. 2008.

**Kunli Zhou** was born in Chongqing, China, on September 5, 1989. He received the B.E. degree from Sichuan University, Chengdu, China, in 2011. He is currently working toward the Ph.D. degree in the Department of Electrical Engineering, Tsinghua University, Beijing, China, and at the National Institute of Metrology, Beijing, China.

His research interests include noise thermometry and quantum voltage standards.

**Jifeng Qu** was born in Xi'an, China, on December 16, 1978. He received the B.S. degree in materials physics and the Ph.D. degree in condensed matter physics from the University of Science and Technology of China, Hefei, China, in 2001 and 2006, respectively.

In April 2007–October 2009, he was a Guest Researcher on the Johnson Noise Thermometry Program at the National Institute of Standards and Technology, Boulder, CO, USA, where he investigated electronic nonlinearities using superconducting quantum-based voltage sources. In November 2009, he joined the National Institute of Metrology, Beijing, China, where he is currently working on Josephson voltage standards and quantum-voltage-calibrated Johnson noise thermometry.

**Samuel P. Benz** (M'01–SM'01–F'10) was born in Dubuque, IA, USA, on December 4, 1962. He received the B.A. degree (*summa cum laude*) in physics and math from Luther College, Decorah, IA, USA, in 1985 and the M.A. and Ph.D. degrees in physics from Harvard University, Cambridge, MA, USA, in 1987 and 1990, respectively.

In 1990, he joined the National Institute of Standards and Technology (NIST), Boulder, CO, USA, as a NIST/National Research Council Postdoctoral Fellow, and in January 1992, he became a permanent Staff Member. Since October 1999, he has been the Project Leader of the Quantum Voltage Project at NIST. He has worked on a broad range of topics within the field of superconducting electronics, including Josephson junction array oscillators, single-flux quantum logic, ac and dc Josephson voltage standards, Josephson waveform synthesis, and noise thermometry. He is the author or coauthor of over 160 publications, and he is the holder of 3 patents in the field of superconducting electronics.

Dr. Benz is a Fellow of the American Physical Society and a member of Phi Beta Kappa and Sigma Pi Sigma. He was the recipient of three U.S. Department of Commerce Gold Medals for Distinguished Achievement and the 2006 IEEE Council on Superconductivity Van Duzer Prize. He was also the recipient of the R. J. McElroy Fellowship (1985–1988) during his Ph.D. studies.